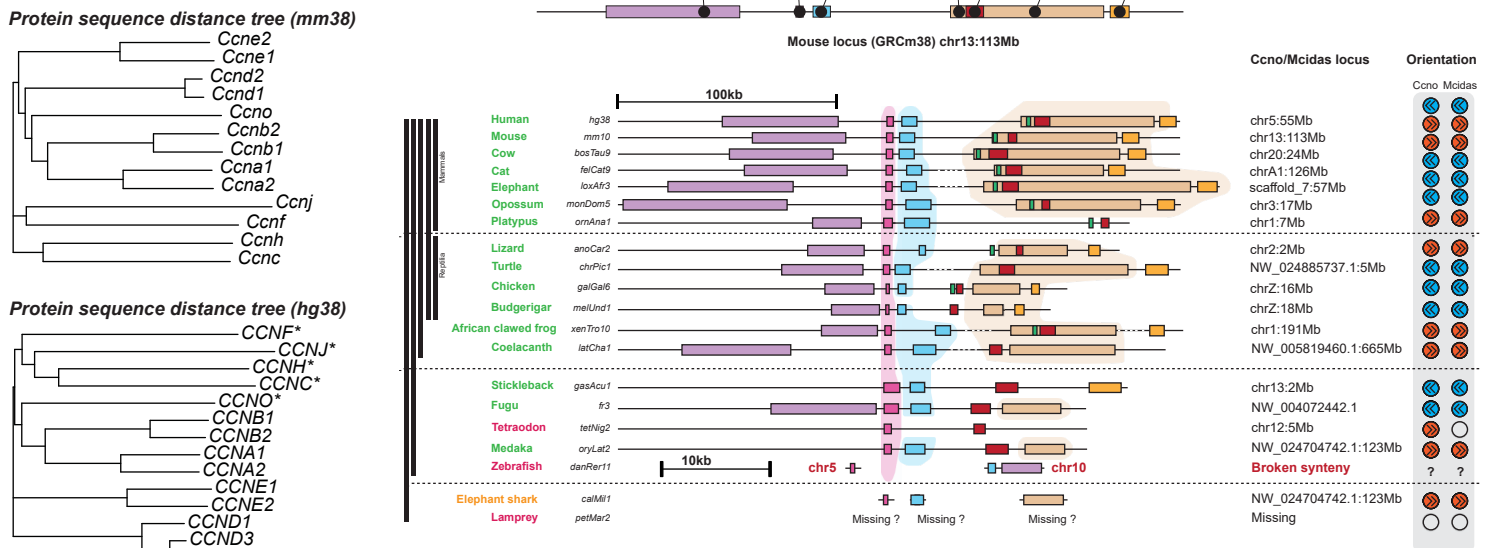
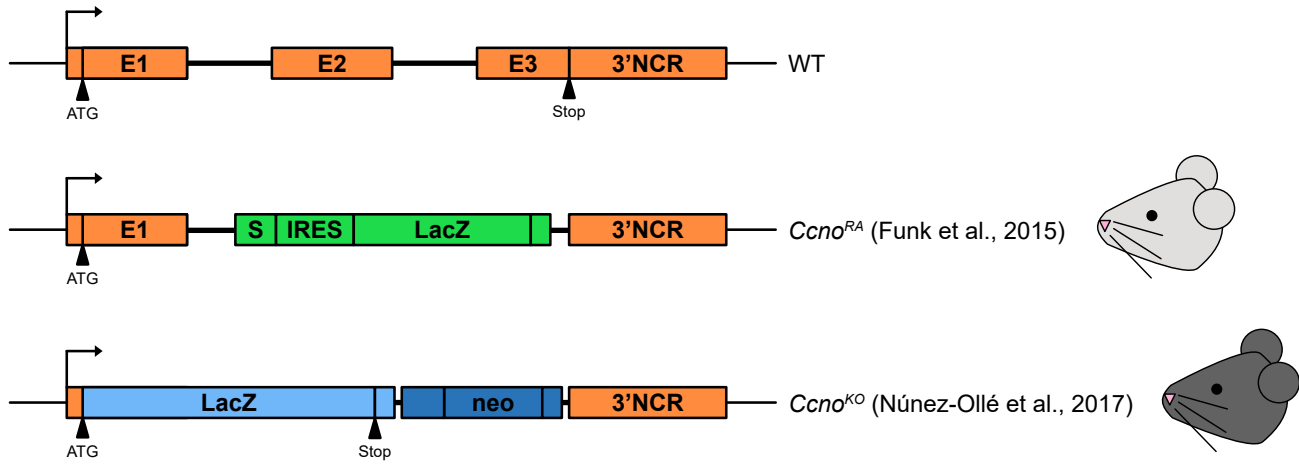
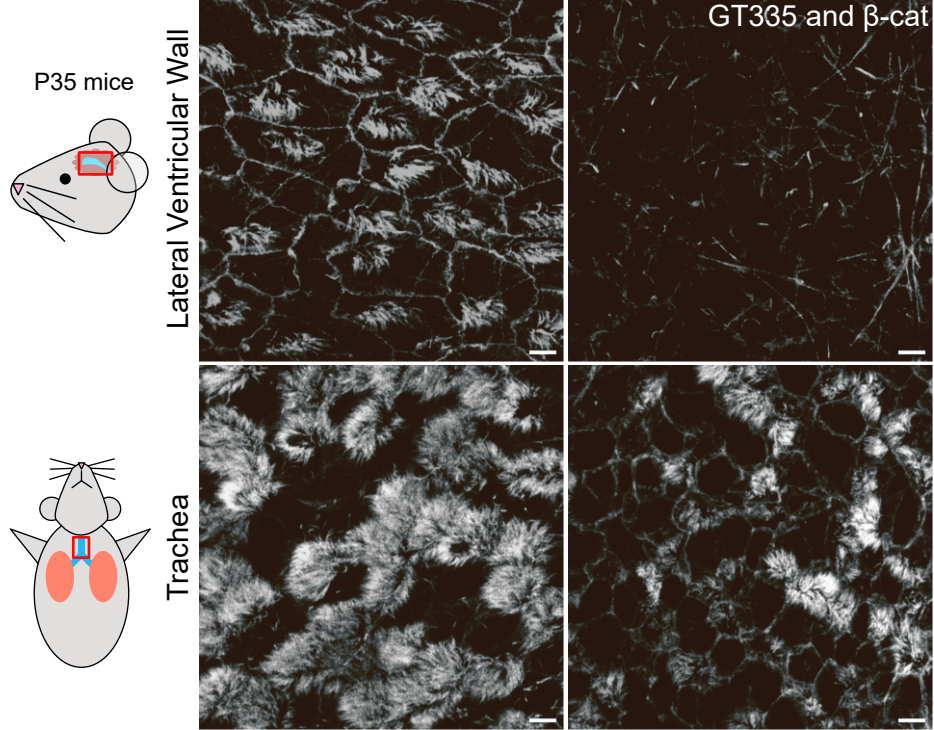


**Supplemental information**

**Cyclin O controls entry  
into the cell-cycle variant required  
for multiciliated cell differentiation**

**Michella Khoury Damaa, Jacques Serizay, Rémi Balagué, Amélie-Rose Boudjema, Marion Faucourt, Nathalie Delgehyr, Kim Jee Goh, Hao Lu, Ee Kim Tan, Cameron T. James, Catherine Faucon, Rana Mitri, Diana Carolin Bracht, Colin D. Bingle, Norris Ray Dunn, Sebastian J. Arnold, Laure-Emmanuelle Zaragosi, Pascal Barbry, Romain Koszul, Heymut Omran, Gabriel Gil-Gómez, Estelle Escudier, Marie Legendre, Sudipto Roy, Nathalie Spassky, and Alice Meunier**

**A****B****C****Figure S1**

**Figure S1 – Mutated *Ccno* progenitors fail to develop into MCC in the mouse brain compared to the mouse trachea, related to Figure 1.**

- (A) Phylogeny of CCNO protein in both mouse and human and conservation of CCNO gene locus among various species.
- (B) *Ccno* gene alleles in WT, *Ccno*<sup>KO</sup> and *Ccno*<sup>RA</sup> mouse lines. *Ccno*<sup>RA</sup> has two exons removed and *Ccno*<sup>KO</sup> has all exons removed.
- (C) Immunostaining of LVW and trachea dissected from a single *Ccno*<sup>RA</sup> or WT individual at P35 for cilia (GT335) and β-cat, showing a complete lack of MCC in the LVW and a decrease of MCC in the trachea, similar to what is observed in *Ccno*<sup>KO</sup>. Images shown from one representative experiment. Scale bar 5μm.

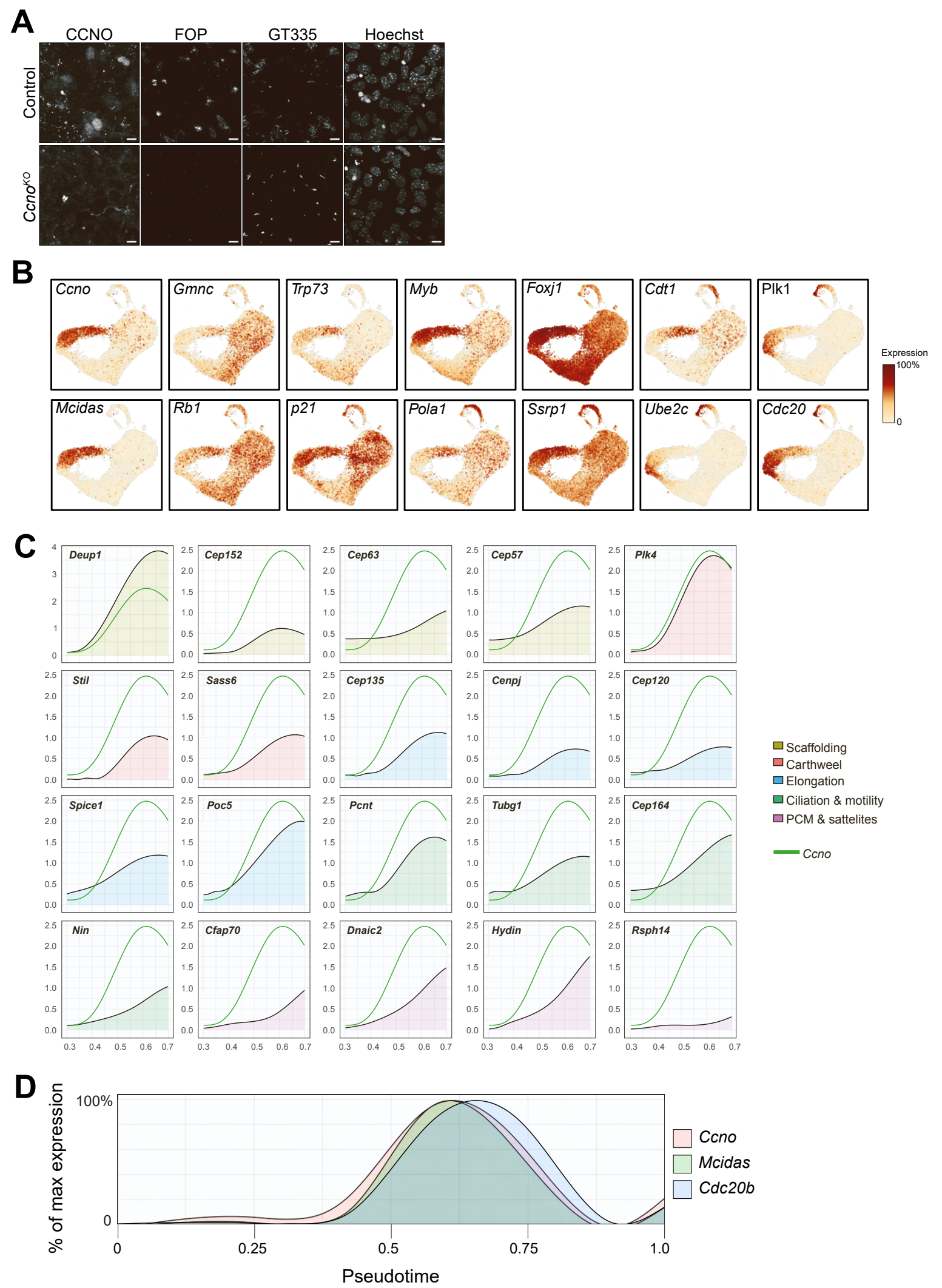


Figure S2

**Figure S2 – Cyclin O is expressed at the onset of MCC differentiation, MCC cell cycle variant and MCC centriole amplification, related to Figure 2.**

- (A) Validation of CCNO antibody in *Ccno*<sup>KO</sup> cultured ependymal cells at DIV2. Images shown from one representative experiment where several control and *Ccno*<sup>KO</sup> mice were pooled together in culture. Scale bar 10μm.
- (B) UMAP plots of gene expression listed in Fig. 2H-I-J
- (C) Expression of various genes involved in centriole biogenesis and ciliation compared to *Ccno* expression along differentiation pseudotime.
- (D) Expression of *Ccno*, Mcidas and *Cdc20b* along differentiation pseudotime.

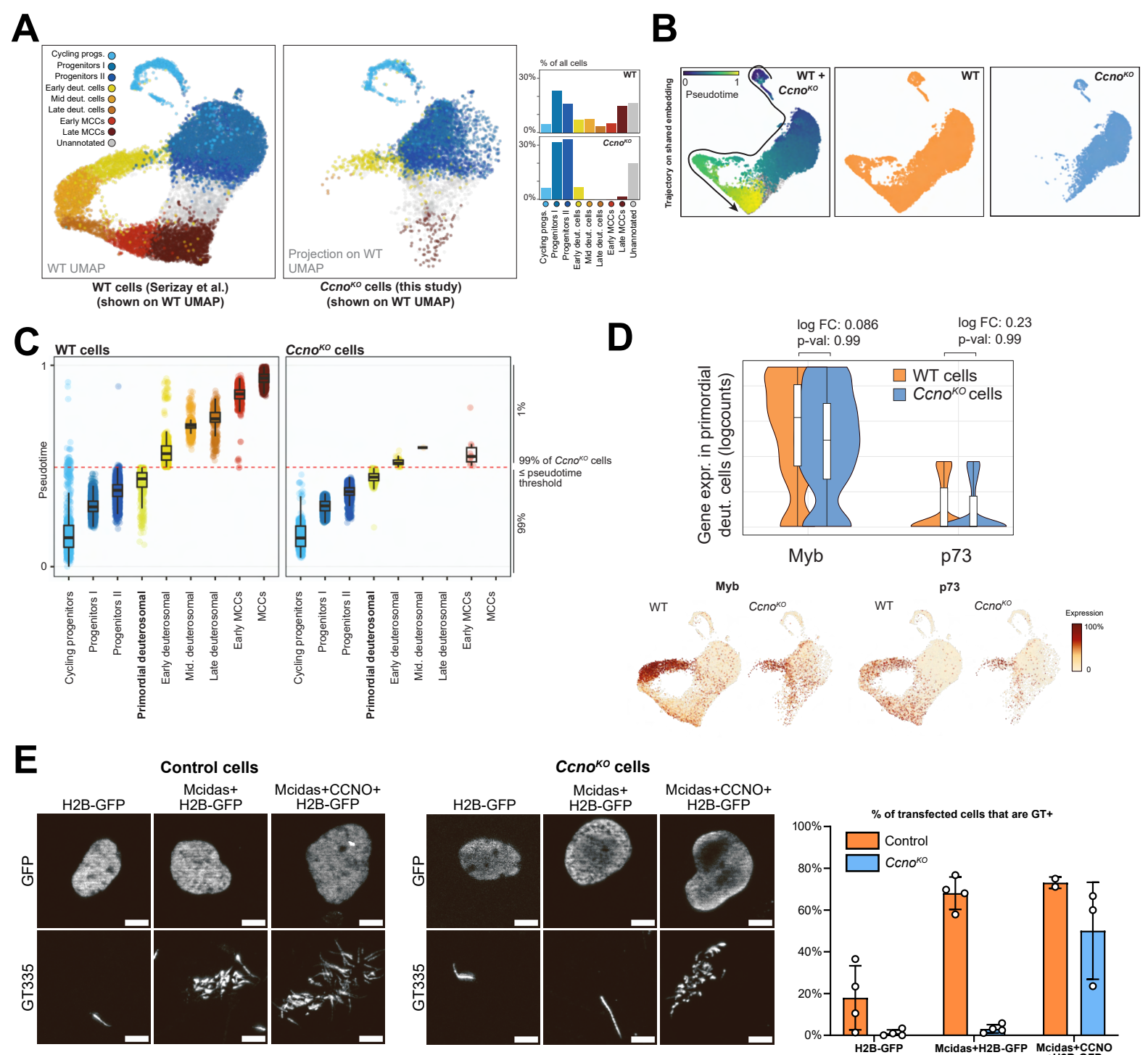


Figure S3

**Figure S3 – CCNO is required for the early progression of MCC differentiation, related to Figure 3**

- (A) UMAP projections of WT and *Ccno*<sup>KO</sup> scRNAseq datasets, with annotations transferred from Serizay et al., 2024.
- (B) Lineage inference and pseudotime computation of combined WT and *Ccno*<sup>KO</sup> datasets.
- (C) Thresholding of pseudotime used to determine the primordial deuterosomal cluster. Boxplots show the median pseudotime values (horizontal line), the interquartile range (IQR; represented by the height of the box, spanning from the 25th to the 75th percentile), and the whiskers extend from the box to the smallest and largest values within 1.5 times the IQR from the lower and upper quartiles, respectively.
- (D) Expression of MCC differentiation factors *Myb* and *p73* in primordial deuterosomal cells from WT and *Ccno*<sup>KO</sup> samples. Both genes are expressed at comparable levels in WT and *Ccno*<sup>KO</sup>. Boxplot representations are as in (C).
- (E) Transfection of control and *Ccno*<sup>KO</sup> cells by MCIDAS or MCIDAS+CCNO, followed by GT335 immunostaining at DIV5. Scale bar 5 $\mu$ m. Each singular point represents an independent experiment carried on cultured ependymal cells of various control and *Ccno*<sup>KO</sup> mice that were pooled together. Columns represent the average quantification and error bars represent standard deviation.

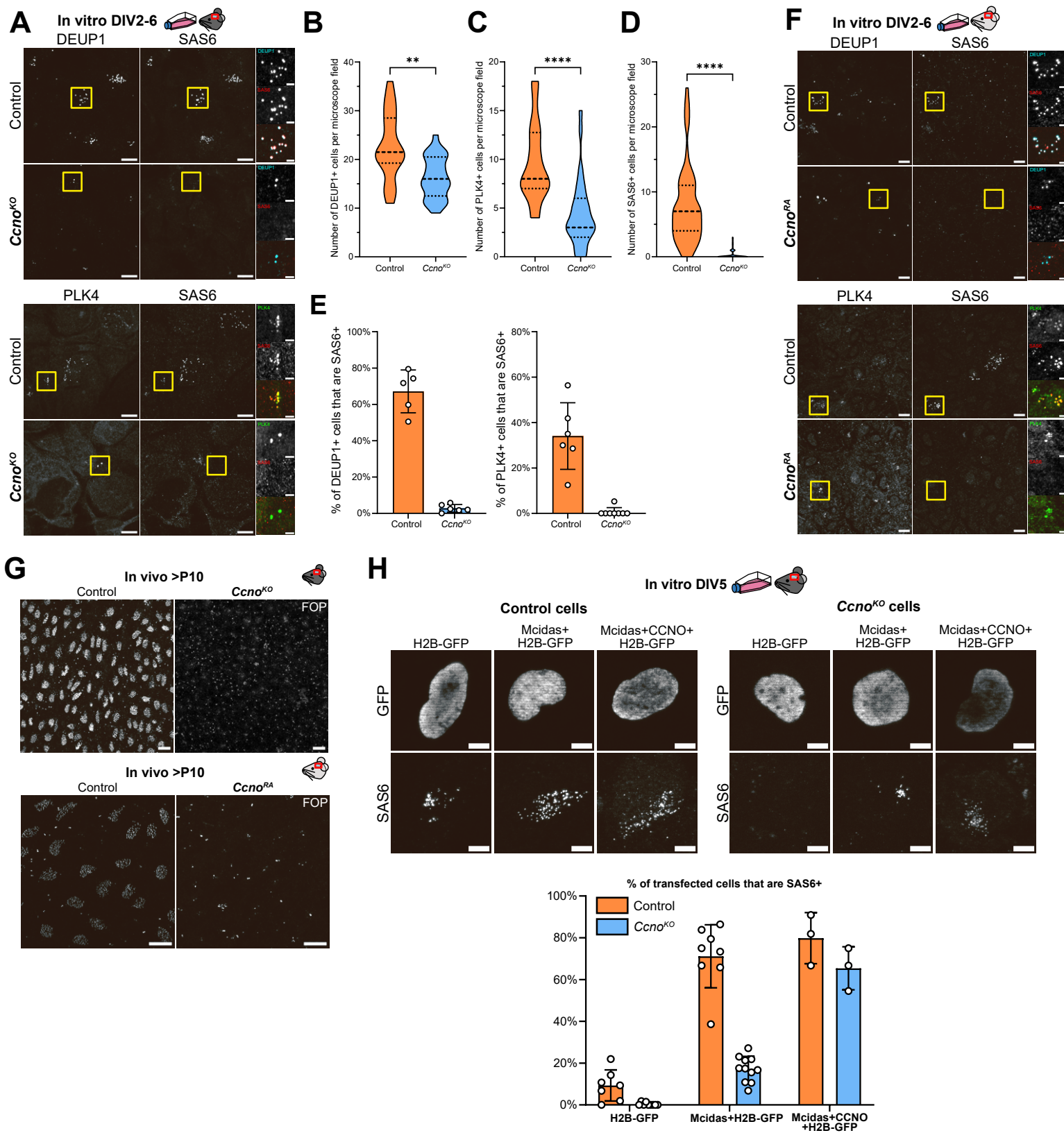
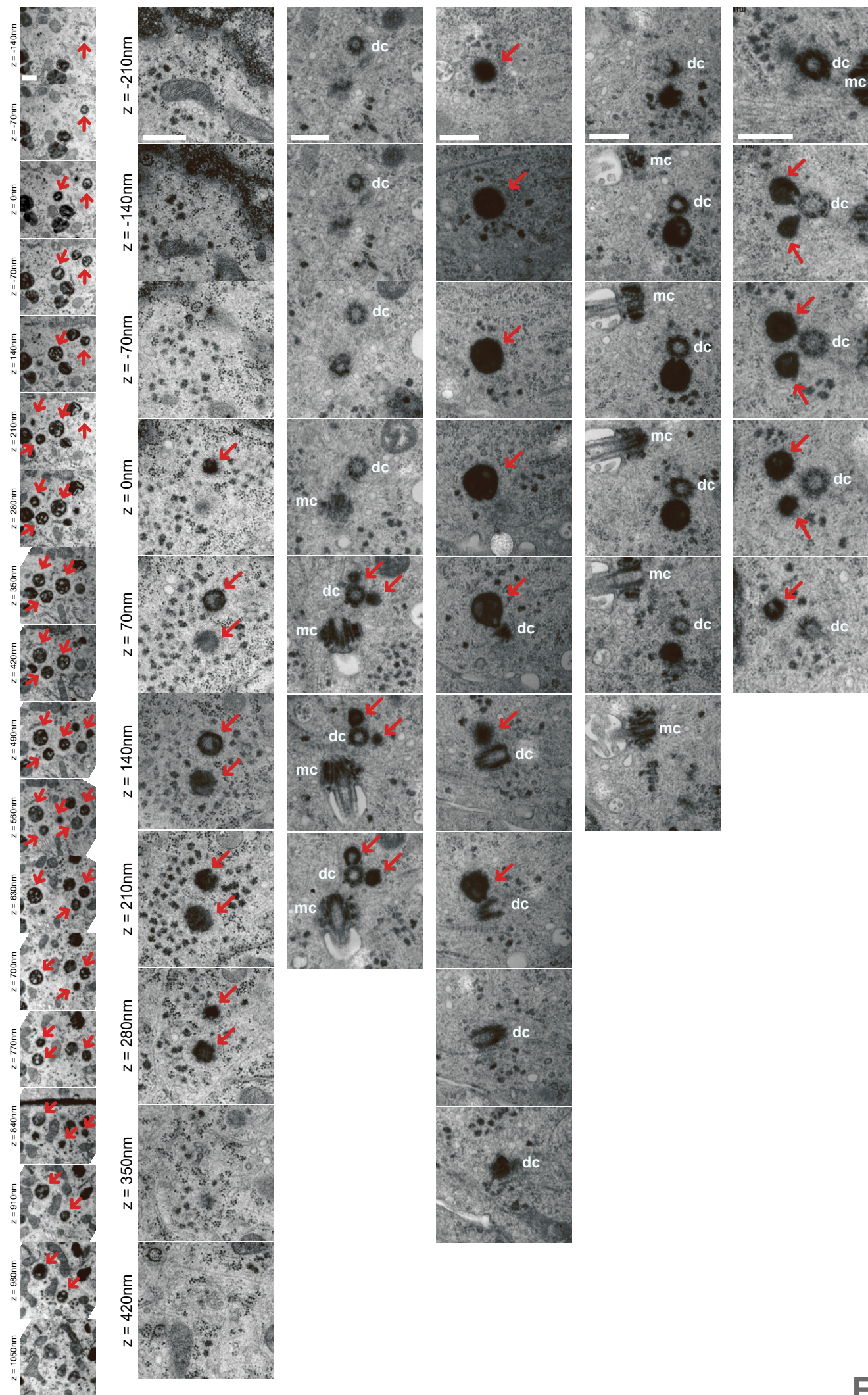


Figure S4

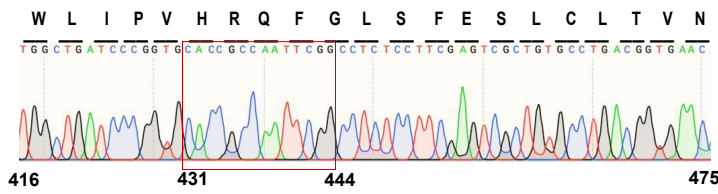
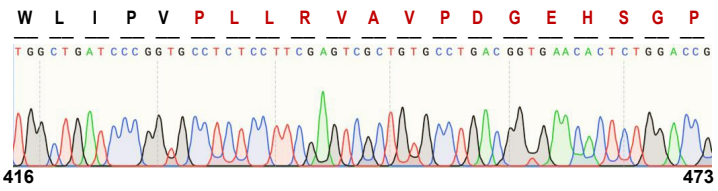
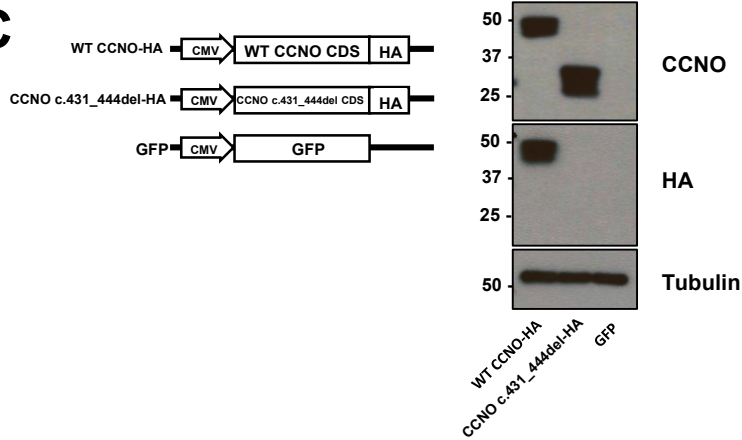
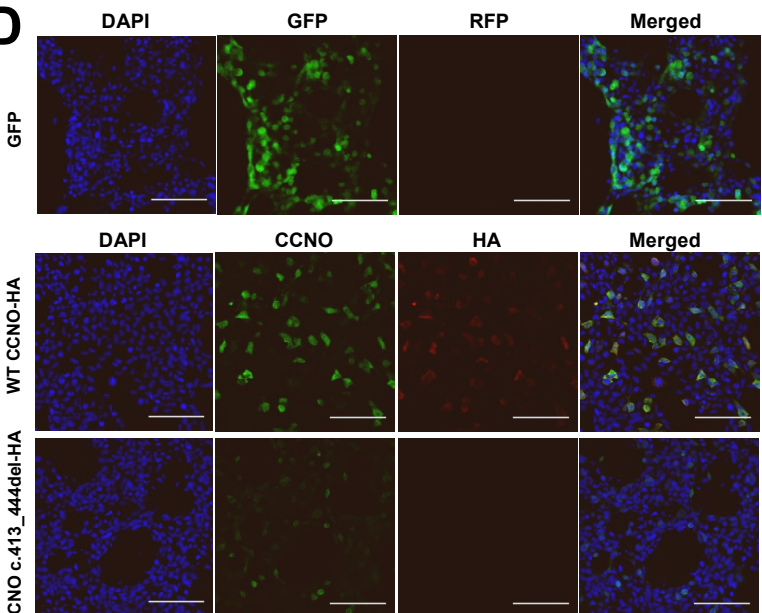
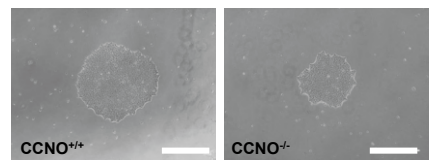
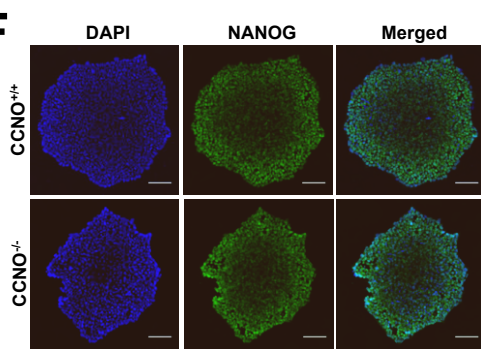
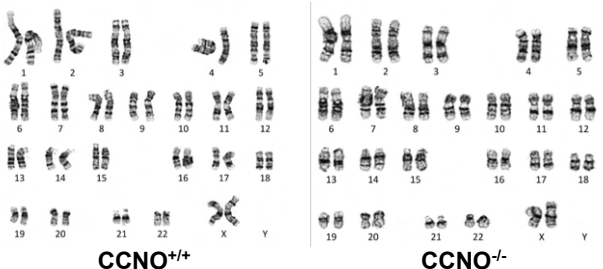
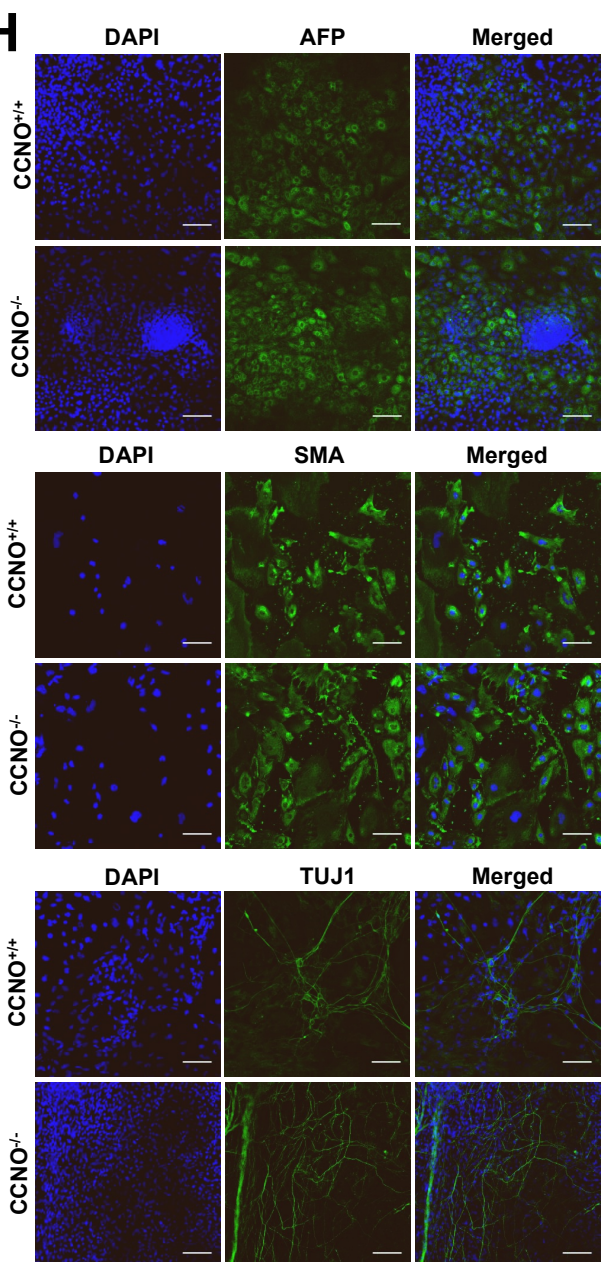
**Figure S4 – Absence of CCNO blocks centriole amplification at the onset of centriole biogenesis, related to Figure 5**

- (A) Immunostaining of in-vitro cultures at ages between DIV2 and DIV6 for DEUP1, PLK4 and SAS6. *Ccno*<sup>KO</sup> cells are able to express DEUP1 and PLK4 but not SAS6. Scale bar 10µm for large field images and 2,5µm for zoom-ins.
- (B) Quantification of the number of DEUP1+ cells in microscope field in Control and *Ccno*<sup>KO</sup> in vitro. Images from 5 control mice and 6 *Ccno*<sup>KO</sup> mice were quantified, with 4 images per cultured coverslip, Control: 20 values *Ccno*<sup>KO</sup>: 25 values. P-values derived from two-tailed Mann-Whitney U-test, \*\*p-value=0.0013. The violin plots represent the distribution of values, the dashed horizontal line shows the median value, and the dotted horizontal lines show the interquartile range.
- (C) Quantification of the number of PLK4+ cells in microscope field in Control and *Ccno*<sup>KO</sup> in vitro. Images from 6 control mice and 8 *Ccno*<sup>KO</sup> mice were quantified, with 4 images per cultured coverslip, Control: 24 values *Ccno*<sup>KO</sup>: 31 values. P-values derived from two-tailed Mann-Whitney U-test, \*\*\*\*p-value<0.0001. Data are represented as (B).
- (D) Quantification of the number of SAS6+ cells in microscope field in Control and *Ccno*<sup>KO</sup> in vitro, showing that *Ccno*<sup>KO</sup> fail to express SAS6. Images from 12 control mice and 12 *Ccno*<sup>KO</sup> mice were quantified that were previously used for either PLK4 or DEUP1 quantification with 4 to 8 images per cultured coverslip, Control: 68 values *Ccno*<sup>KO</sup>: 75 values. P-values derived from two-tailed Mann-Whitney U-test, \*\*\*\*p-value<0.0001. Data are represented as (B).
- (E) Quantification of the proportion of DEUP1+ cells and PLK4+ cells that are able to express SAS6 in both WT and *Ccno*<sup>KO</sup> in vitro. One point represents an animal, from the same dataset used to quantify DEUP1, PLK4 and SAS6 number of cells. Columns represent the average quantification and error bars represent standard deviation.
- (F) Immunostaining of in-vitro cultures of *Ccno*<sup>RA</sup> at DIV3 for DEUP1, PLK4 and SAS6. *Ccno*<sup>KO</sup> cells are able to express DEUP1 and PLK4 but not SAS6. Representative images taken from one experiment. Scale bar 10µm for large field images and 2,5µm for zoom-ins.
- (G) Immunostaining of in-vivo controls and *Ccno*<sup>KO</sup> or *Ccno*<sup>RA</sup> lateral ventricles (>P10) for basal bodies, marked by FOP. Representative images taken from one experiment for each. Scale bar 10µm.
- (H) MCIDAS overexpression in *Ccno*<sup>KO</sup> partially rescue SAS6 expression. Controls and *Ccno*<sup>KO</sup> cultured ependymal cells are transfected with plasmid(s) coding for H2B-GFP, H2B-GFP+MCIDAS or H2B-GFP+MCIDAS+CCNO at DIV-1, and immunostained at DIV5 for SAS6 and GFP. Scale bar 5µm. Each singular point represents an independent experiment carried on cultured ependymal cells of various control and *Ccno*<sup>KO</sup> mice that were pooled together. Columns represent the average quantification and error bars represent standard deviation.

**Figure S5**

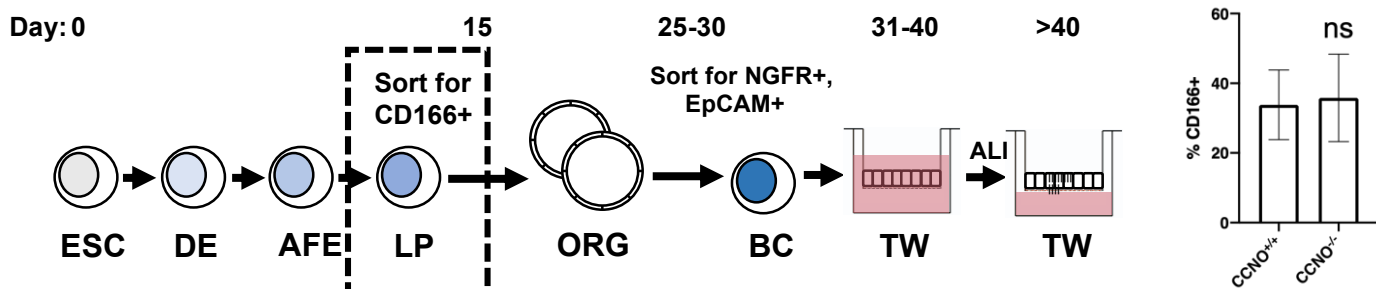
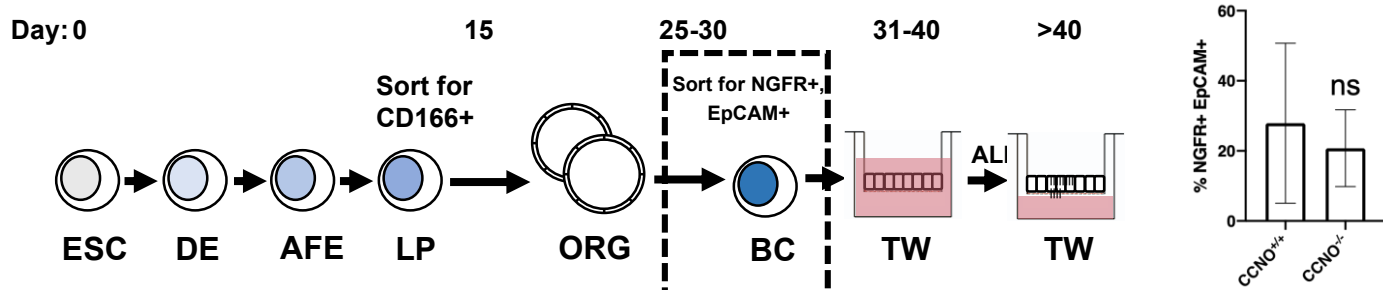
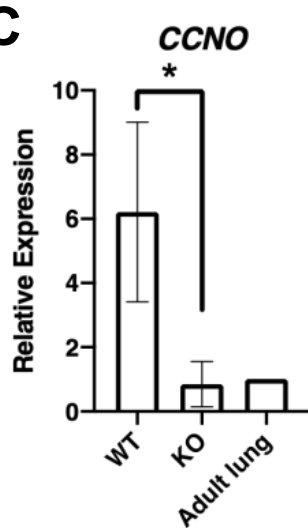
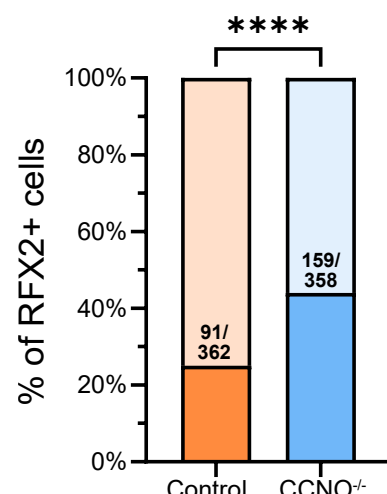
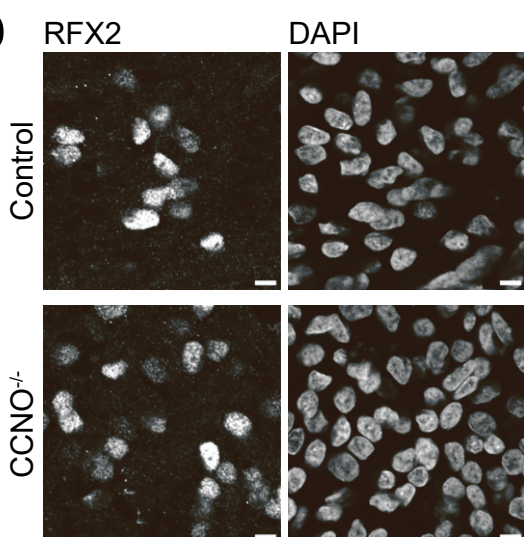


**Figure S5 - Electron microscopy images show enlarged and empty deuterosomes with no procentrioles in *Ccno<sup>RA</sup>* cells, related to Figure 5.** Serial ultra-thin sections of cell from *Ccno<sup>RA</sup>* cells at DIV5 showing empty deuterosomes in the cytoplasm, or connected to the daughter centriole of the centrosome. Images from one representative experiment of cultured ependymal *Ccno<sup>RA</sup>* cells from several mice pooled together. Deuterosomes are indicated by red arrows. mc: mother centriole of the centrosome, dc: daughter centriole of the centrosome. Scale bar 0,5μm.

**A** *CCNO***B** *CCNO<sup>+/+</sup>**CCNO<sup>-/-</sup>***C****D****E****F****G****H****Figure S6**

**Figure S6 – Generation and validation of  $CCNO^{-/-}$  H9 ESCs, related to Figure 6.**

- (A) Schematic of gene editing strategy. gRNA3 was selected which targets exon 2 of the *CCNO* gene.
- (B) Sanger sequencing of the *CCNO* gene in  $CCNO^{+/+}$  and  $CCNO^{-/-}$  cells. Red box indicate the 14 bp sequence deletion found in the  $CCNO^{-/-}$  cells.
- (C) Western blotting of CCNO or HA in HEK293T cells overexpressing HA-tagged wild type (WT) and mutant CCNO cDNA sequences. Tubulin was used as a loading control. GFP-overexpressing HEK293T cells was used as a negative control.
- (D) Representative images of HEK293T cells overexpressing HA-tagged wild type (WT) and mutant CCNO cDNA sequences immunostained for CCNO or HA. GFP-overexpressing HEK293T cells was used as a negative control.
- (E) Brightfield images of representative  $CCNO^{+/+}$  and  $CCNO^{-/-}$  ESC colonies.
- (F) Representative images of  $CCNO^{+/+}$  and  $CCNO^{-/-}$  ESC immunostained for pluripotency marker NANOG.
- (G) Karyotype analysis of  $CCNO^{+/+}$  and  $CCNO^{-/-}$  ESCs.
- (H) Trilineage differentiation of  $CCNO^{+/+}$  and  $CCNO^{-/-}$  ESCs followed by immunostaining of markers specific to the 3 germ layers: AFP (endoderm), SMA (mesoderm) and TUJ1 (ectoderm).

**A****B****C****D****Figure S7**

**Figure S7 – Stepwise differentiation of CCNO<sup>+/+</sup> and CCNO<sup>-/-</sup> ESCs into airway epithelial cells, related to Figure 6.**

**(A)** Schematic of differentiation protocol. Black box indicates when cells were sorted and assessed for % CD166 expression in lung progenitors (LP). Columns represent the average quantification and error bars represent standard deviation.

**(B)** Schematic of differentiation protocol. Black box indicates when cells were sorted and assessed for % NGFR;Ep-CAM expression in proximal lung organoids (ORG). Columns represent the average quantification and error bars represent standard deviation.

**(C)** QPCR analysis of proximal airway epithelial cell markers. n=3. Expression was normalized to adult lung cDNA.

\*p <0.05. Student's t test. Columns represent the average quantification and error bars represent standard deviation.

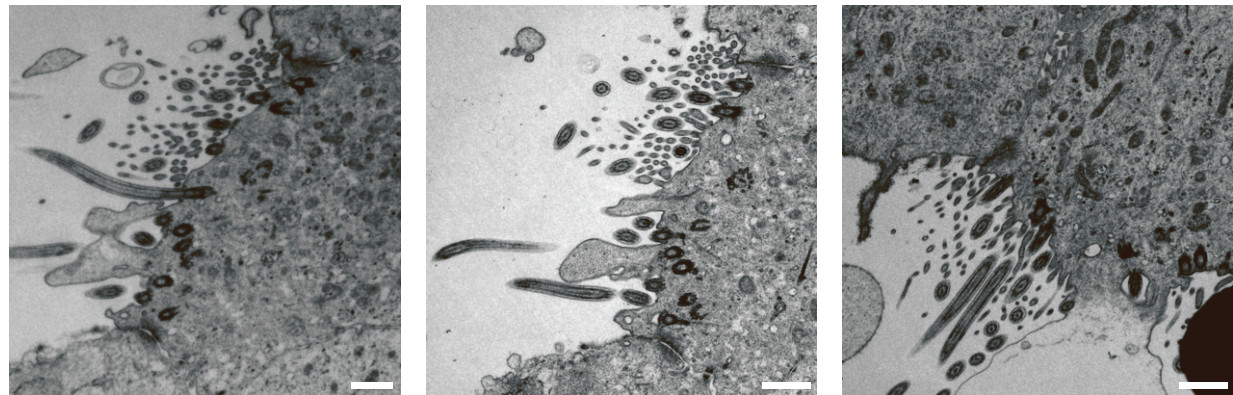
**(D)** RFX2 expression in control vs CCNO<sup>-/-</sup> ESCs differentiated into airway epithelial cells. Scale bar 5 $\mu$ m. P-values derived from two-sided Chi-square test (two-proportion z-test), \*\*\*p-value<0.0001.

**A**

CCNO patient	Total cells	Cells with aggregates	Cells with cytoplasmic rootlets	Cells with more than 2 BB/cilia
L	6	0	0	0
M	3	0	1	2
N	4	0	0	0
O	4	3	0	0
P	1	1	0	0
Q	7	1	2	0
R	4	2	3	0
S	1	0	0	0
T	3	0	0	0

**B**

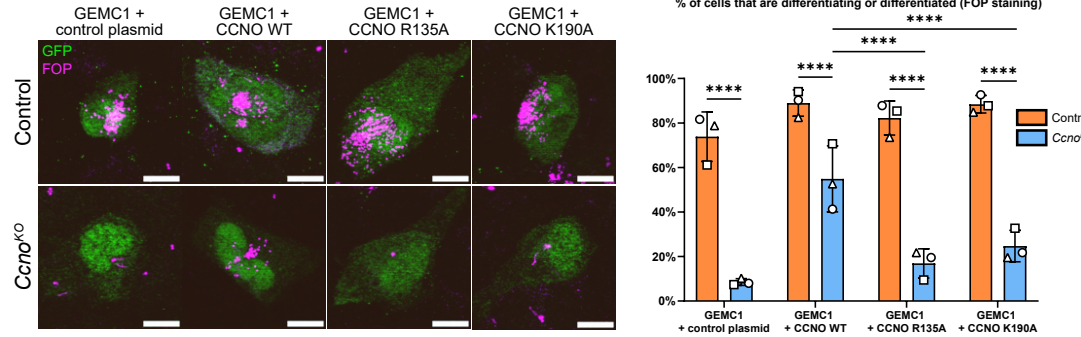
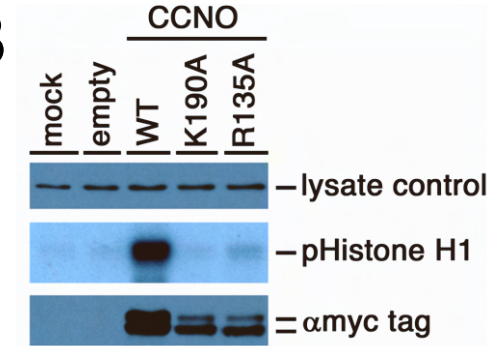
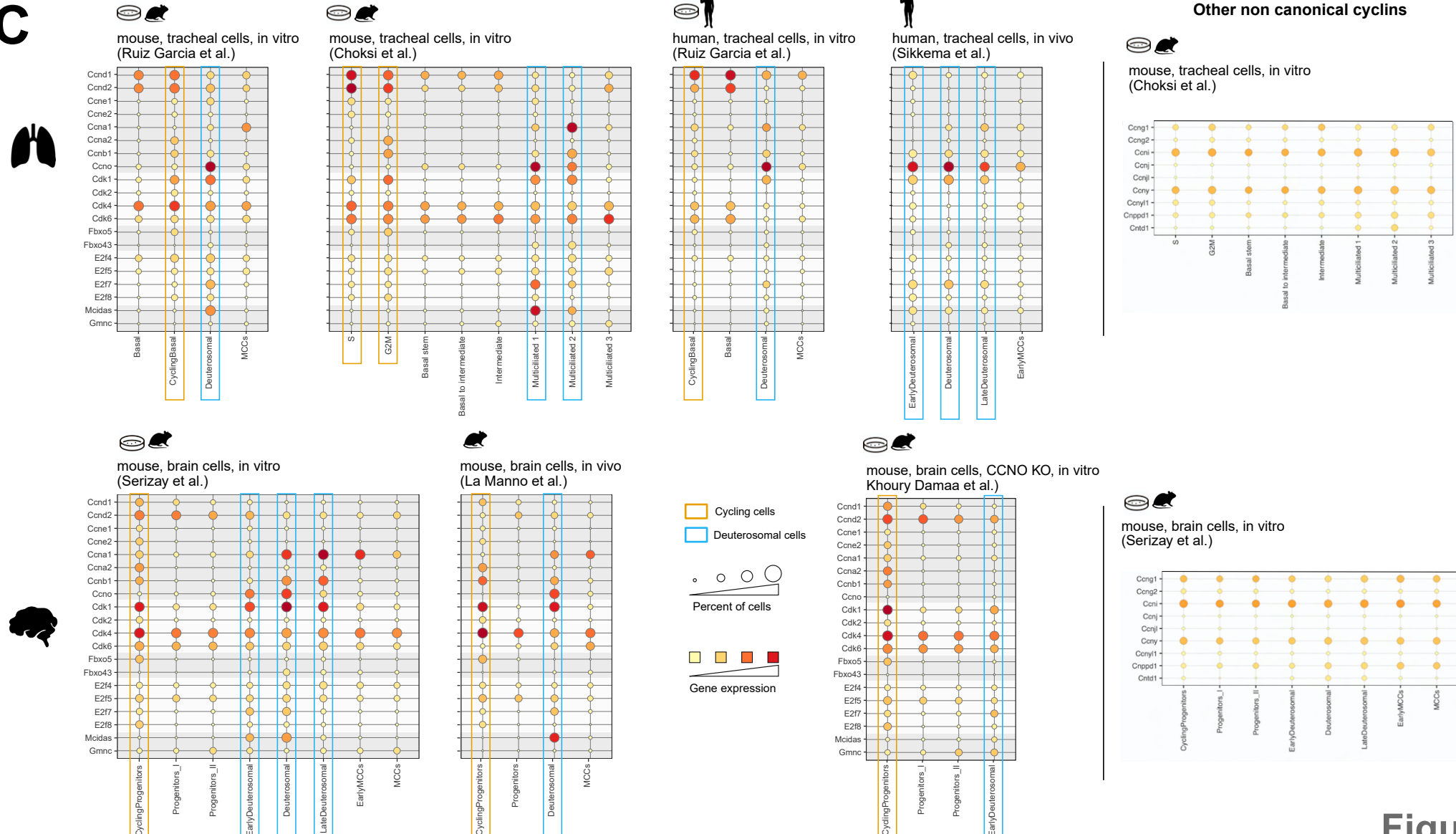
CCNO patient H



**Figure S8 – Transmission electron microscopy images of CCNO human patients, related to Figure 6.**

(A) Quantification of numbers of cells that have rootlets, aggregates and more than two basal bodies and/or cilia in CCNO patients listed.

(B) TEM images of the 3 cells (out of 53) from CCNO patient H showing multiple basal bodies and/or cilia. Scale bar 1 $\mu$ m.

**A****B****C****Figure S9**

**Figure S9 – *Ccno*<sup>KO</sup> phenotype cannot be rescued by a CDK-dead version of CCNO and comparison of expression of different cell cycle factors in different MCC tissues from mouse and human, related to Figure 7.**

(A) Rescue or not of the *Ccno*<sup>KO</sup> phenotype by overexpression of GEMC1 and control plasmid Linker B, CCNO in native form (CCNO WT) or mutated in their areas of potential interaction with CDKs (CCNO R135A and CCNO K190A, see methods). Transfected cells are labelled with the GFP contained in the plasmids used (green) and the centrioles are marked by FOP (magenta). Scale 10 μm. Quantification of the percentage of cells that are differentiating or are differentiated among the cells transfected with the different plasmid combinations. Each singular point represents an independent experiment carried on cultured ependymal cells of various control and *Ccno*<sup>KO</sup> mice that were pooled together. Each symbol represents an independent experiment. Cultures used were quantified between DIV3 and DIV5. P-values derived from two-sided Chi-square test (two-proportion z-test), \*\*\*\*p-value<0.0001. Columns represent the average quantification and error bars represent standard deviation.

(B) Measurement of the kinase activity of the anti-myc tag immunoprecipitates formed after expression of myc-tagged CCNO WT, CCNO R135A or CCNO K190A in HEK293 cells using Histone H1 as substrate (see methods). Upper gel: cell lysate control. Middle gel: Histone H1 IP+kinase assay after transient transfection of the indicated proteins. Lower gel: WB against the 9E10 anti-myc tag antibody.

(C) The expression of different cell cycle factors involved in MCC differentiation (cyclins, Cdks, Emi1/Fbxo5, Emi2/Fbxo43, E2f factors) and non-canonical cyclins is shown for different cell populations in mouse or human brain or respiratory MCC differentiating cells. The dynamics of re-expression of the main cell cycle factors in mouse brain or mouse and human respiratory MCC are mainly comparable. Notably, (i) the expression of CCNO instead of E-type cyclins, except for mouse respiratory cells where E-type cyclins are still expressed, (ii) the expression of Ccna1 instead of Ccna2, (iii) the re-expression of D-type cyclins and Ccnb1 (iv) the silencing of Emi1/Fbxo5 replaced by a mild expression of Emi2/Fbxo43, (v) re-expression of E2F4/5/7/8 except for E2F4/5 in human, (vi) re-expression of Cdk1, (vii) re-expression of Cdk4/6 except in human MCC, (viii) absence of detection of Cdk2, (ix) massive expression of Mcidas and (x) difficult detection of Gmnc which can be detected very late during the differentiation process. No obvious difference is observed in the expression of non-canonical cyclins between mouse brain and tracheal MCCs.

**Table S1 - Genotypes and phenotypes of control PCD patients, related to Figure 6.**

Individuals (Ancestry, age at molecular diagnosis)	Gene Genotype	Known Consanguinity	Gender	Laterality defect	Airway Disease	nNO	HSVA (CBF)	TEM defects
A, 18GM01423 (South Asia, 38 yrs)	<i>DNAH5:</i> c.841_842insCTTCCGC p.(Val281Alafs*20) homozygous	Yes	Female	No	NNRD Bronchitis Bronchiectasis Rhinosinusitis Nasal polyposis Otitis media	Low <sup>§</sup>	Immotile cilia	ODA
B, 20GM000711 (France, 18 yrs)	<i>DNAH5:</i> c.2710G>T p.(Glu904*) c.9897+1del p.? compound heterozygous	No	Female	Yes	NNRD Bronchitis Bronchiectasis Rhinosinusitis Otitis media	Low <sup>§</sup>	NA	ODA & IDA
C, 22GM000288 (France, 38 yrs)	<i>CCDC39:</i> c.2347_2351delTTTCA p.(Phe783Thrfs*3) homozygous	No	Male	No	NNRD Bronchitis Bronchiectasis Rhinosinusitis Otitis media	Low <sup>§</sup>	Dyskinetic and immotile cilia	IDA with MTD
D, 20GM000324 (Sub-Saharan Africa, 35 yrs)	<i>CCDC39:</i> c.876del p.(Lys292Asnfs*16) c.2158+5del p.? compound heterozygous	No	Male	No	Bronchitis Bronchiectasis Rhinosinusitis Serious otitis	Low <sup>§</sup>	Dyskinetic cilia	IDA with MTD

E, 18GM00086 (Caribbean, 77 yrs)	<i>DNAH11:</i> c.11182dup p.(Leu3728Profs*10) homozygous	No	Female	Yes	Bronchitis Bronchiectasis Rhinosinusitis Serious otitis	Low <sup>§</sup>	Immotile cilia	Normal ultrastructure
-------------------------------------	---	----	--------	-----	--	------------------	----------------	--------------------------

**Table S2 - Genotypes and phenotypes of patients with *CCNO* pathogenic variations, related to Figure 6.**

Individual (Ancestry, age at molecular diagnosis)	<i>CCNO</i> Genotype	Known Consanguinity	Gender	Airway Disease	nNO
F, 19GM00243 (North Africa, 17 yrs)	c.248_252dup p.(Gly85Cysfs*11) homozygous	Yes	Male	NNRD Bronchitis Bronchiectasis Rhinosinusitis Otitis media Mild developmental delay	Low <sup>§</sup>
G, 19GM00351 (France, 8 yrs)	c.337G>A p.(Glu113Lys) c.592A>T p.(Lys198*) compound heterozygous	No	Male	NNRD Bronchitis Bronchiectasis Rhinosinusitis Otitis media Inborn deafness	Low <sup>§</sup>
H, 18GM01179 (France, 7 yrs)	c.248_252dup p.(Gly85Cysfs*11) c.793dup p.(Val265Glyfs*106) compound heterozygous	No	Male	NNRD Bronchitis Bronchiectasis Rhinosinusitis Otitis media	Low <sup>§</sup>
I, 19GM01068 (Turkey, 9 yrs)	c.258_262dup p.(Gln88Argfs*8) homozygous	Yes	Male	NNRD Bronchitis Rhinosinusitis Otitis media	NA

<b>J</b> , OP-1246 III (Germany, 14 yrs) [S1]	c.258_262dup p.(Gln88Argfs*8) rs587777499 homozygous	Yes	Male	NNRD Recurrent pneumonia Bronchitis Rhinitis Cough	NA
<b>K</b> , OP-642 II1 (Germany, 23 yrs) [S1]	c.926del p.(Pro309Argfs*18) homozygous	Yes	Female	NNRD Otitis media Sinusitis Recurrent pneumonia Bronchitis	Low <sup>§</sup>
<b>L</b> , OI-66 II1 (Israel, 41 yrs) [S2]	c.638T>C; p.(Leu213Pro) homozygous	Yes	Male	NNRD Bronchiectasis recurrent pneumonia Otitis Sinusitis Cough	Low <sup>§</sup>
<b>M</b> , OI-104 II1 (Israel, 58 yrs) [S2]	c.258_262dup p.(Gln88Argfs*8) rs587777499 homozygous	No	Male	Bronchiectasis Recurrent pneumonia Cough	NA
<b>N</b> , OP-151 II1 (Austria, 31 yrs) [S1]	c.258_262dup p.(Gln88Argfs*8) rs587777499 homozygous	No	Male	NNRD Recurrent pneumonia Rhinitis Cough	Low <sup>§</sup>
<b>O</b> , OP-971 II1 (Germany, 25 yrs) [S1]	c.716A>G p.(His239Arg) homozygous	Yes	Female	NNRD Recurrent pneumonia Bronchiectasis Otitis media	NA

<b>P</b> , OP-1367 II1 (Germany, 24 yrs) [S1]	c.258_262dup p.(Gln88Argfs*8) rs587777499 homozygous	Yes	Male	NNRD Recurrent pneumonia Rhinosinusitis Bronchiectasis Otitis media Cough	NA
<b>Q</b> , OP-1777 I5 (Kuwait, NA) [S1]	c.248_252dup p.(Gly85Cysfs*11) rs587777498 homozygous	NA	Female	NA	NA
<b>R</b> , OP-1777 II1 (Kuwait, NA) [S1]	c.252_253insTGCCC p.(Gly85Cysfs*10) homozygous	NA	Male	NA	NA
<b>S</b> , OP-1777 II2 (Kuwait, NA) [S1]	c.248_252dup p.(Gly85Cysfs*11) rs587777498 homozygous	NA	Female	NA	NA
<b>T</b> , OP-1977 III1 (Germany, 26 yrs)	c.258_262dup p.(Gln88Argfs*8) rs587777499 homozygous	NA	Male	Middle lobe atelectasis Bronchiectasis Rhinitis Cough	Low <sup>s</sup>

: <77nL/min; nNO: nasal nitric oxide; TEM: transmission electron microscopy; NNRD: neonatal respiratory distress; NR: non relevant (child); NA: not assessed; ODA: outer dynein arm defect; IDA: inner dynein arm defect; MTD: microtubular disorganization

## Supplemental references list

- [S1] Boon, M.; Wallmeier, J.; Ma, L.; Loges, N. T.; Jaspers, M.; Olbrich, H.; Dougherty, G. W.; Raidt, J.; Werner, C.; Amirav, I.; Hevroni, A.; Abitbul, R.; Avital, A.; Soferman, R.; Wessels, M.; O'Callaghan, C.; Chung, E. M. K.; Rutman, A.; Hirst, R. A.; Moya, E.; Mitchison, H. M.; Van Daele, S.; De Boeck, K.; Jorissen, M.; Kintner, C.; Cuppens, H.; Omran, H. MCIDAS Mutations Result in a Mucociliary Clearance Disorder with Reduced Generation of Multiple Motile Cilia. *Nat Commun* **2014**, *5*, 4418. <https://doi.org/10.1038/ncomms5418>.
- [S2] Amirav, I.; Wallmeier, J.; Loges, N. T.; Menchen, T.; Pennekamp, P.; Mussaffi, H.; Abitbul, R.; Avital, A.; Bentur, L.; Dougherty, G. W.; Nael, E.; Lavie, M.; Olbrich, H.; Werner, C.; Kintner, C.; Omran, H.; Investigators, I. P. C. Systematic Analysis of CCNO Variants in a Defined Population: Implications for Clinical Phenotype and Differential Diagnosis. *Human Mutation* **2016**, *37* (4), 396–405. <https://doi.org/10.1002/humu.22957>.